Published 03/28/2017

doi:10.4271/2017-01-0723
saeeng.saejournals.org

Optimization of an Advanced Combustion Strategy Towards 55% BTE for the Volvo SuperTruck Program

Jacqueline O'Connor, Meghan Borz, Daniel Ruth, Jun Han, Chandan Paul, Abdurrahman Imren, and Daniel Haworth
Pennsylvania State University

Jonathan Martin and Andre Boehman
University of Michigan

Jian Li, Kevin Heffelfinger, Samuel McLaughlin, Richard Morton, Arne Andersson, and Anders Karlsson
Volvo Group Trucks Technology

ABSTRACT

This paper describes a novel design and verification process for analytical methods used in the development of advanced combustion strategies in internal combustion engines (ICE). The objective was to improve brake thermal efficiency (BTE) as part of the US Department of Energy SuperTruck program. The tools and methods herein discussed consider spray formation and injection schedule along with piston bowl design to optimize combustion efficiency, air utilization, heat transfer, emission, and BTE. The methodology uses a suite of tools to optimize engine performance, including 1D engine simulation, high-fidelity CFD, and lab-scale fluid mechanic experiments. First, a wide range of engine operating conditions are analyzed using 1-D engine simulations in GT Power to thoroughly define a baseline for the chosen advanced engine concept; secondly, an optimization and down-select step is completed where further improvements in engine geometries and spray configurations are considered. Next, simultaneous high-fidelity simulation using StarCD and OpenFOAM as well as lab-scale unsteady jet mixing experiments are used to understand the interplay between fuel injection and piston bowl designs. A key to the success of this design and analysis process is the accuracy of both the 1-D and high-fidelity simulations; these tools have been significantly improved and benchmarked against a range of engine operating conditions throughout the program. We conclude by outlining future directions for this methodology.

CITATION: O'Connor, J., Borz, M., Ruth, D., Han, J. et al., "Optimization of an Advanced Combustion Strategy Towards 55% BTE for the Volvo SuperTruck Program," *SAE Int. J. Engines* 10(3):2017, doi:10.4271/2017-01-0723.

INTRODUCTION

This paper describes a design and analysis process developed as part of the Department of Energy SuperTruck program [1]. The SuperTruck program outlined a number of goals for improvement of vehicle efficiency, including demonstration of a 50% increase in freight efficiency (ton-miles per gallon) as compared to a 2009 baseline vehicle, achievement of a 50% brake thermal efficiency (BTE) in a new heavy-duty diesel engine, and identification of a pathway that identifies a 55% BTE engine. This work focuses on the development of the "pathway" to 55% BTE, in which the Department of Energy required the use of modeling and analysis to identify "critical components and/or systems needing specific development to achieve this goal."

A thorough review of the limiting factors and potential areas for improving the engine's efficiency using analytical simulations was performed. The preliminary assessment included alternative thermodynamic cycles and new engine design concepts. The final assessment of the chosen engine concept measured against the 55% efficiency goal included the additional gains expected from the use of a Rankine waste heat recovery system, optimized auxiliaries, and reduced friction losses.

There are a number of significant challenges in achieving 55% BTE in a commercially viable engine. Both mechanical and thermodynamic aspects of an ICE must be optimized to achieve these high values. Designing engines that will achieve ambitious efficiency and emissions goals requires the use of tools capable of simulating new engine operation regimes. Volvo and partners took a holistic approach in improving the tools that guide engine design by employing new methods for analysis and combining them with traditional methods of simulating aspects of engine operation.

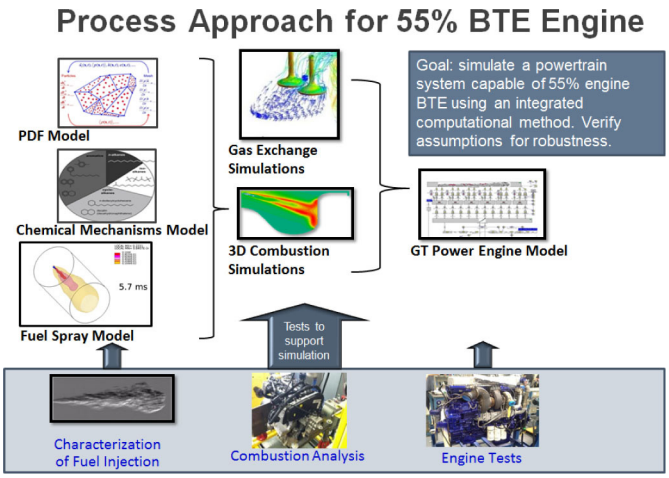

Figure 1. Key steps in the process development towards 55% BTE.

For example, as indicated in Figure 1, a process flow that relies on traditional tools and data has been combined with an analytical approach capable of determining the output of new hardware and combustion phenomena. The complex characterization of fuel injection was achieved via the combination of fuel mechanisms, computational fluid dynamics (CFD) and the continued development of Volvo's in-house fuel spray model which was corroborated by lab-scale fluid mechanics experiments. Secondly, combustion analysis included a separate study of the gas exchange process along with a parametric review of in-cylinder combustion parameters. This combustion analysis also included a robust comparison of standard mRIF (multiple Representative Interactive Flamelet) CFD techniques that were aligned with the transported probability density function (PDF) method discussed later. The final, high fidelity results were then input into a developed GT Power model to gain BTE as an output.

This paper describes the pathway by which the Volvo SuperTruck team, including partners from Volvo, the Pennsylvania State University, and the University of Michigan, achieved a 55% BTE concept through the development of high-fidelity tools that supported the design of an advanced combustion strategy. In particular, the result of the effort is a set of tools that were verified using a unique combination of low- and high-fidelity simulation, scaled laboratory experiments, and prior baseline engine test results. The pathway to 55% BTE outlined by the Volvo SuperTruck team provided modeling, analysis, and experimental verification of the models, to support the proposed pathway. While these tools were developed in support of the SuperTruck program, we will show that they can be used to understand a range of advanced combustion strategies.

The remainder of this paper describes the design process and provides details about the tools and their verification. The result of this effort is a methodology that can be used to design combustion strategies outside the bounds of normally-validated models. First, we provide an overview of the design and analysis process developed to show the connectivity between simulation, analysis, and experiment. Next, we detail each step of the process, using example results from analyses of different components to highlight the importance of these steps towards achieving the Department of Energy goals. Finally, we discuss the implications of this process for the design of next generation engines.

OVERVIEW OF THE DESIGN PROCESS

The design process and tool verification effort consisted of a feedback loop between various simulations and experiments. Figure 2 provides an overview of this process.

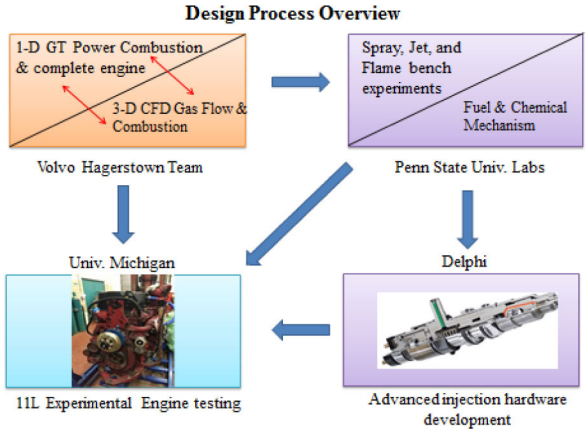

Figure 2. Feedback loop depiction of the design process through experimental and simulation collaboration between partners.

In a step-wise procedure, the Volvo team utilized both, 1-D complete engine and 3-D combustion/gas flow simulations to work in parallel to develop a series of broad spectrum design of experiments (DOE) that were used to validate and facilitate downstream lab and bench level tests. These DOEs are filtered for key engine operation parameters that can be verified using conventional engine test cell data, backed with previously calibrated simulations. As these DOEs were post processed, they were evaluated for consistent and agreeable trends towards the 55% BTE goal, where a selected group of parameter values were used to further develop tools, experiments, and hardware downstream. The results of the detailed 3-D parameter analysis aided in the selection of engine hardware to be used in future experiments.

These selected key parameter values were then passed to the team at the Pennsylvania State University where further testing was done to validate the 1-D/3-D simulations loop in a scaled gas jet experiment. Parallel high fidelity simulation was also carried out in order to provide continued agreement with both the 1-D and 3-D engine and combustion simulations. While many of the key engine parameters for fuel injection, combustion, and heat transfer need continued investigation, other parameters (engine speed, torque, start of injection, etc.) were correlated and analyzed with respect to baseline engine data.

After validation and selection of the remaining parameter values from the tests and simulation were concluded, the final fuel injection strategy and hardware development process began with the partners at Delphi. Advanced fuel injector, rail, pump, nozzle tip, and software were developed based on the results of the previous design process loop steps. With the collected combination of developed hardware,

bench experiments, and simulation parameter validation, future testing at the University of Michigan will include a series of fired single cylinder engine cell tests, dedicated to validating the design process described here.

DETAILS OF THE DESIGN PROCESS

The goal of the design process was to simultaneously optimize piston bowl shape, fuel injection, and operating gas exchange conditions, in order to maximize efficiency within reasonable emissions limits. Traditional limits of compression ignition combustion were stretched, resulting in a larger design space. In particular, we considered a large number of intake conditions, high peak cylinder pressures, and nontraditional injection timings to maximize both power and efficiency.

To accomplish this, 1-D GT-Power simulations were carried out to parametrically evaluate the 55% BTE engine performance, with a Volvo internal predictive combustion model implemented in GT-Power. The 1-D GT-Power simulations predicted the engine performance and provided the boundary conditions for the 3-D CFD simulations. Generally, the design of experiment function in GT-Power was used to run detailed engine evaluations at a variety of different operating conditions, in order to define the relationships between controlling quantities and input variables. The best engine performance points were then selected from the DOE results at a variety of different engine speeds and loads. The DOE results can provide the steady conditions such as mass of trapped charge, and pressure/temperature boundaries to the 3-D CFD simulations, which significantly simplifies the analysis for the initial simulations. The 3-D simulations in return provided the heat release, heat transfer, and emission calculations to correct the 1-D simulation assumptions as depicted in Figure 3.

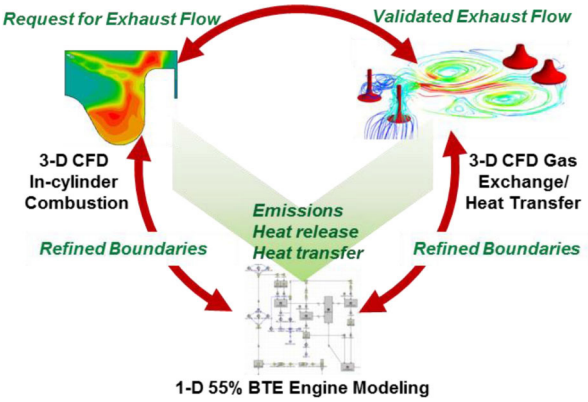

Figure 3. Methodology of Volvo 55% BTE engine concept evaluation and optimization.

Preliminary Engine Performance Screening

Comprehensive 1-D engine performance screening was carried out in order to investigate the brake thermal efficiency potential of the chosen Volvo 55% BTE engine concept. A number of engine speed key points varying from 900 rpm to 1800 rpm were simulated by sweeping the air-fuel equivalence ratio, EGR rate, rail pressure, and injection timing, respectively, as shown in Figure 4.

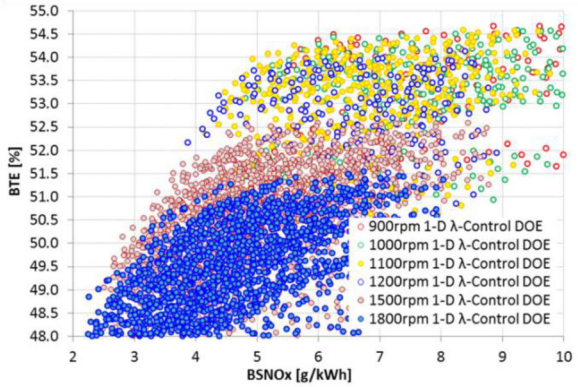

Figure 4. Trade-offs of BTE vs. BSNOx from 55% BTE engine performance screening based on air-fuel equivalence ratio sweep.

The trade-off of BTE and BSNOx from the lambda controlled design of experiments studies in Figure 4 indicates the best potential performance with the maximum brake torque occurs at a lower range of the engine speed, 900 rpm – 1200rpm. Thus additional 1-D engine performance screening was carried out at a selected engine speed of 1200 rpm and air-fuel equivalence ratio 1.3, varying from brake torque of 740 Nm up to 1550 Nm, by sweeping EGR rate, fuel rail pressure and injection timing, respectively, as shown in Figure 5.

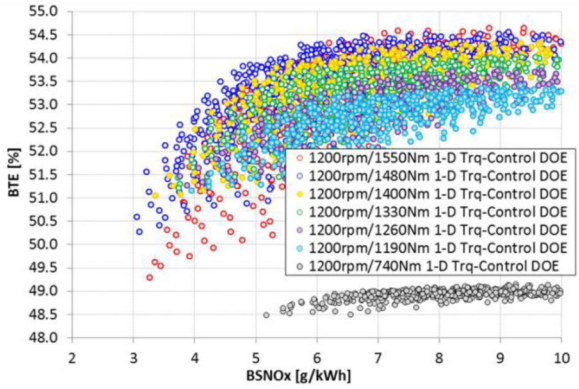

Figure 5. Trade-offs of BTE vs. BSNOx from 55% BTE engine performance screening based on brake torque control sweep.

The brake torque controlled DOE studies in Figure 5 indicate the optimum potential performance of the BTE-BSNOx trade-offs up to 54.0% with the peak cylinder pressure constraint of 300 bar at BSNOx of 8 g/kWh.

Parameter Space Down-Select

With the results of parameter space exploration completed, a further parameter space down-select was done to further reduce the number of cases to explore using higher fidelity tools. This simulation process was done using Volvo in-house multidimensional CFD modeling, including spray modeling and combustion modeling. The Lagrangian VSB2 spray model [2] is based on the idea of constructing a model that treats the spray and its breakup as one process, instead of summing individual, fragmenting droplets to a spray. The VSB2

model, with its proven stability and practically no tuning parameters, is well-suited for engine simulations covering large variations in engine operating conditions. The model used for thermodynamics and combustion is the mRIF combustion model. Initially developed at RWTH Aachen [3], the model assumes that a typical diffusion flame consists of a large number of very small laminar flames stretched by turbulence through the scalar dissipation rate. The scalar dissipation rate varies by orders of magnitude in the cylinder, particularly along the spray. One way to overcome this problem is to solve for more than one flamelet and couple each with its own fuel tracer, then average the scalar dissipation rate only in the zones that the tracer currently occupies. Thus, the mRIF model uses different flamelets in different parts of the spray. In the case where flamelets overlap in space, the feedback to the CFD solver, e.g. local mean of temperature, is tracer weighted from different flamelet solutions. The ideal gas law is the equation of state and the Sutherland viscosity law is employed. The turbulence model is the standard k-ε model, and the Star-CD solver from CD-Adapco is used for the simulations.

Piston Bowl Optimization

The combustion chamber design is critical to the overall performance of the heavy duty diesel engine. Changes to this portion of the system can dramatically affect the efficiency and emissions of the engine. One way to change the combustion process in the chamber is to modify the injection spray/piston bowl interaction. This change can be accomplished through modification of the design of both the injector nozzle and piston bowl. The process of changing and optimizing the design of these components and their interaction can be analytically streamlined by using modeling and engine testing in concert. The present work proposes to improve engine efficiency and validate the combustion chamber design through this approach. A number of piston bowl shapes for 55% BTE engine concepts were proposed, designed to enhance the flame recirculation and mixing paired with high swirl ratio conditions. 3-D CFD combustion simulations were carried out in order to investigate the influence on heat release and emissions from the bowl shapes and selected injection configurations.

Figure 6 demonstrates the combustion analysis based on the 3-D CFD simulation results of in-cylinder combustion with baseline piston bowl and proposed piston bowl option 2, respectively. The calculated rate of apparent heat release against crank angle during injection and combustion processes are compared to indicate improved heat release in the early combustion stage, caused by enhanced fuel-air mixing by fluid motions to dominate the combustion process in the chamber. The re-entrant shape forms stronger flame recirculation to improve the mixing process to speed up the combustion, and the bowl diameter is tuned for optimum spray-wall impingement timing. The apparent heat release rate predicted by the combustion CFD was then fed back to 1-D engine modeling. The coupled 1-D/3-D simulation results indicate the proposed piston bowl option 2 improved BTE by about 0.3% at the selected operating condition (900rpm /1550Nm).

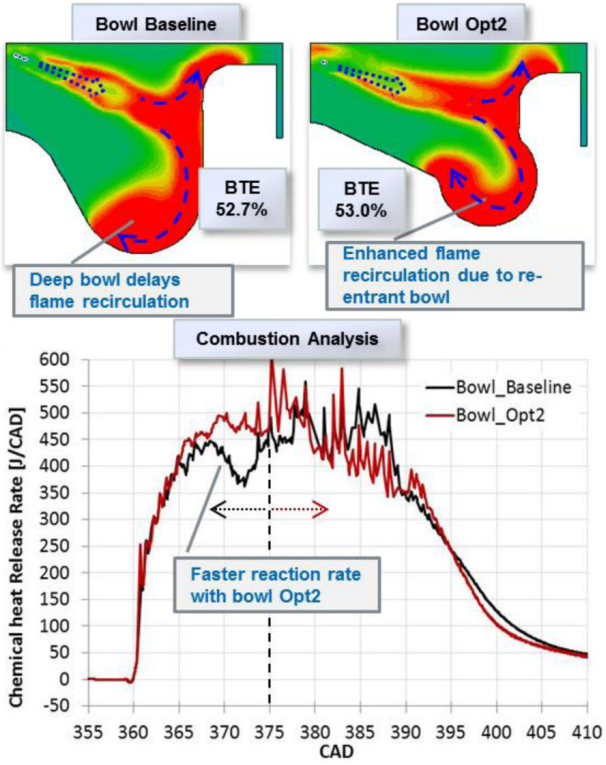

Figure 6. Combustion analysis of piston bowl via 3-D CFD simulations (900rpm /1550Nm).

Gas-Exchange Optimization

The Volvo 55% BTE engine has gained thermal efficiency through improvement of the gas exchange process between cylinders. Preliminary 1-D engine modeling indicated challenges remain in selecting detailed design elements for unconventional engine concepts. When unexpected heat or flow loss were identified by the modeling, new valve and port layouts were created to reduce these losses and achieve optimum volumetric efficiency from gas exchange. Detailed numerical analyses in 3-D Converge CFD were carried out to investigate gas exchange, as demonstrated in Figure 7. The simulated engine conditions were selected from the 1-D simulation results to provide the boundary conditions such as mass of trapped charge, and pressure and temperature boundaries to the 3-D CFD for gas exchange and heat transfer simulations.

The performance optimization of the gas exchange process includes the engine re-compression and the engine performance screening. The engine re-compression tuned the valve timing to gain the optimum pressure phasing during gas exchange. The engine performance screening was also carried out by varying the injection rail pressure, the injection timing, and the EGR rate. The evaluation results in Figure 8 indicate a significant BTE improvement up to 0.6% from gas exchange optimization based on the re-designed exhaust valve/port.

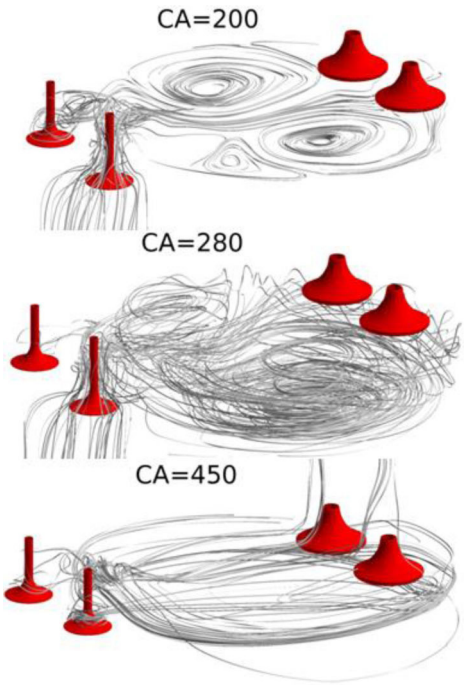

Figure 7. 3-D CFD modeling of gas exchange process.

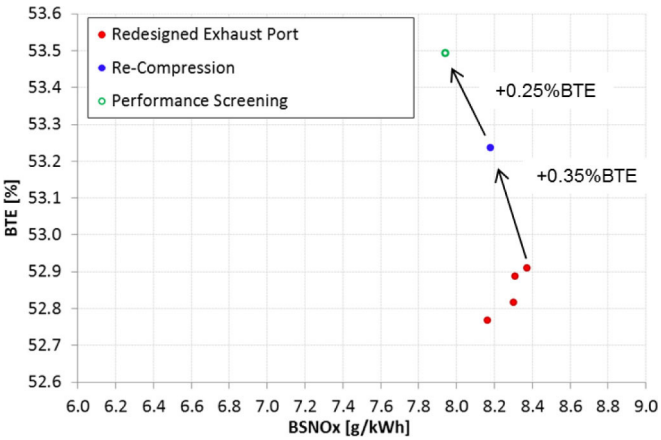

Figure 8. Trade-offs of BTE vs. BSNOx from gas-exchange optimization.

Fuel Injection Strategy

Single injection and multiple injection strategies were explored with a low friction Delphi common rail F3 injector system implemented into the current 55% BTE engine model to evaluate the potential improvements of combustion efficiency and emissions from the split injection strategy. Selected engine key conditions were extracted from the engine re-compression screening results for the fuel injection strategy study.

A number of single and multiple injection strategies varying injection pulse timing and fueling amount were evaluated, focusing on the injection strategy and combustion optimization, coupling 3-D CFD with 1-D engine modeling, as shown in Figure 9. Different pilot injection strategies were employed in order to lower NOx formation, including 5% pilot + 95% main injection, and 10% pilot + 90% main injection. Dwell time between the pilot injection and the main injection varies from 0 CAD up to 50 CAD. 3-D CFD combustion simulations verified a reduction of NOx formation due to the restriction on premixed combustion, and trade-off between IMEP and NOx is optimized regarding the improved tolerance of EGR. The coupled 1-D simulations with 3-D CFD by implementing CFD heat release indicate a maximum BTE up to 54.2% at BSNOx of 8 g/kW-h, with selected engine operating conditions at engine speed 900 rpm and brake torque 1550 Nm.

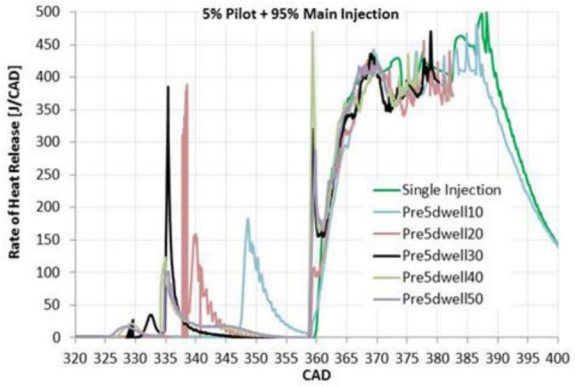

Figure 9. Rate of heat release in multiple injection strategy studies.

55% BTE Engine Concept Performance Evaluation via Coupled 1-D/3-D Modeling

Comprehensive evaluations of the performance of the 55% BTE engine concept have been performed by coupling both 1-D engine modeling and 3-D CFD simulations. Previous engine performance screening achieved the optimum BTE potential up to 54.2% at engine speed 900 rpm and brake torque 1550 Nm, with implementation of Delphi common rail F3 injector system power map and re-designed exhaust valve/port. Further engine performance analysis was then carried out by coupling 1-D GT-Power and 3-D combustion CFD simulations to verify the trade-off of BTE vs. BSNOx at the selected operating conditions 900rpm/1550Nm. Figure 10 compares the heat release rates predicted by the Volvo 1-D engine model and by the 3-D CFD multi-RIF combustion modeling during the power stroke for the 55% BTE engine concept. Although the 1-D Volvo combustion model predicted correct peak cylinder pressure and matched the 3-D CFD calculation well, the rate of heat release curve calculated still missed details of critical combustion events that were actually revealed by the 3-D CFD modeling. By coupling the 1-D engine modeling with the 3-D CFD combustion simulations, the Volvo combustion model in the current 55% BTE engine model was then modified to accommodate a user's input of heat release, extracted from the heat release results by the 3-D CFD simulations.

The methodology using the coupled 1-D GT-Power/3-D CFD simulations redefined the 1-D engine performance screening results, indicating consistent trends of BTE-BSNOx trade-off compared to the 1-D engine modeling results, and lower BTE and higher BSNOx, as shown in Figure 11. The coupled 1-D/3-D simulations brought more accuracy to the final performance and emission evaluations on the latest 55% BTE engine concept model. The validated optimum BTE-BSNOx trade-offs indicate BTE values up to 52.4% at BSNOx of 8.2 g/kWh, as shown in Figure 11.

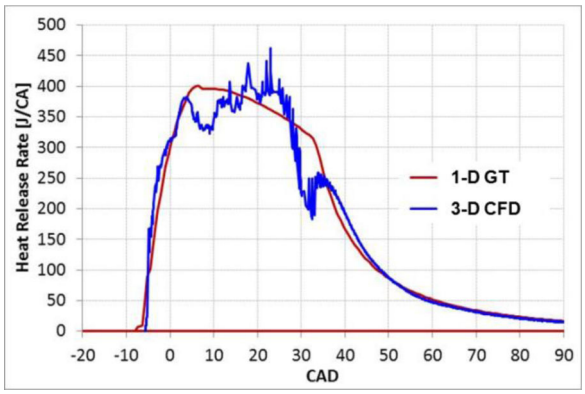

Figure 10. Comparison of heat release rate between 1-D Volvo combustion model and 3-D CFD multi-RIF combustion modeling.

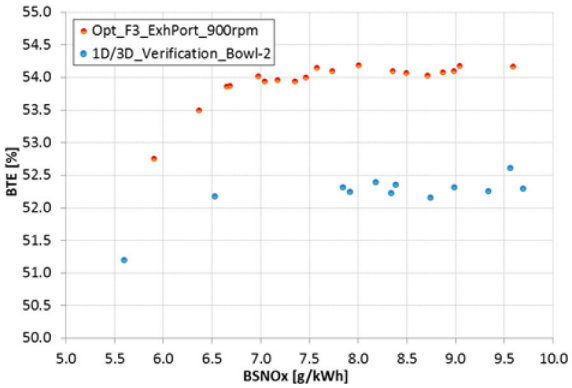

Figure 11. Optimum BTE vs. BSNOx Trade-offs from Coupled 1-D/3-D Modeling optimization.

The final assessment against the 55% efficiency goal includes the additional gains from the reduced friction loss, the use of thermal insulation, and Rankine waste heat recovery system. Higher mechanical efficiency was obtained with very low peak cylinder pressure of the 55% BTE engine cylinder components as the piston rings and bearings can be made with less friction [21]. Low-heat-conductivity and low-heat-capacity material coatings were investigated for thermal insulation of the 55% BTE engine components in the 1-D GT-Power engine modeling. The increased exhaust temperature is then utilized for waste heat recovery using the Volvo Rankine system model, which was calibrated based on SuperTruck 50% BTE engine experiments. Details are not included here, because this paper focuses on the description of the methodology used to design combustion strategies and to develop an analysis process coupling simulations and experiments and their verification.

A Parallel Corroboration of CFD Combustion Analysis

Multidimensional CFD tools were developed and applied over the course of the project to address key issues that arise in advanced turbulent combustion systems for high-efficiency engines. An unsteady RANS framework was adopted, to facilitate running large numbers of parametric studies. Tool development and validation efforts focused on three main aspects: accurate accounting for the influences of unresolved turbulent fluctuations in composition and temperature on autoignition, combustion and emissions; improved spray models to better predict in-cylinder fuel distributions and mixing; and computational strategies to enable the implementation of more realistic chemical mechanisms in engine-scale CFD. The models were implemented in two different CFD codes: a commercial code (STAR-CD [4]) and an open-source code (OpenFOAM [5]). In the remainder of this section, several examples are provided to illustrate the progress in modeling that was made over the course of the project, and to show how the improved CFD tools were applied to meet the 55% BTE objective.

A transported probability density function (PDF) method has been implemented to account for unresolved turbulent fluctuations in composition and temperature [6]. While the merits of PDF methods have been amply demonstrated in laboratory turbulent flames, applications to practical combustion systems have been limited. Here a Lagrangian particle formulation has been adopted to implement PDF-based models in STAR-CD and OpenFOAM, including methods to deal with deforming computational meshes and changing mesh topologies [7].

One important finding from our PDF-based modeling work pertains to the differences in the relative importance of different physical processes in soot formation between atmospheric-pressure combustion versus high-pressure turbulent combustion. Compared to atmospheric-pressure flames (where most soot modeling and experimental studies have been done), it has been found that at engine-relevant pressures, computed soot volume fractions are relatively less sensitive to the kinetic rates in the soot models (because the rates are so fast) and that the rate-limiting processes are turbulent transport and mixing. Accurate accounting for unresolved turbulent fluctuations in composition and temperature is essential.

An example is shown in Figure 12. There the computed and measured total soot mass are plotted as functions of time for ECN Spray A [8]: a transient high-pressure n-dodecane turbulent spray flame. Results from a well-stirred reactor (WSR) model that neglects unresolved turbulent fluctuations in composition and temperature are compared with those from a PDF model that accounts for unresolved turbulent fluctuations, both using the same chemical mechanism and soot model (here a semi-empirical two-equation model). The PDF model shows much better agreement with experiment, especially in capturing the rapid initial transient rise and drop off in soot before a quasi-stationary state is reached. Computed spatial distributions of soot volume fraction are also in much better agreement with experiment for the PDF model (not shown). Similar results were found in a modeling study of a heavy-duty diesel engine over a range of operating conditions [7]. In that study, with all other aspects of the models being the same, computed engine-out soot levels from a PDF model were higher (by orders of magnitude, in some cases) than those from a WSR model, and the PDF results were in much closer agreement with experiment (Figure 13).

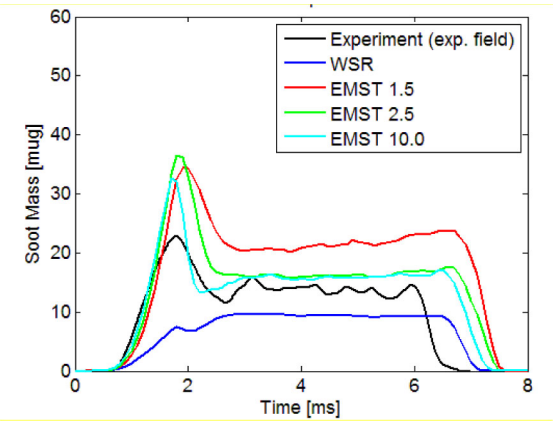

Figure 12. Computed and measured total soot mass as a function of time for ECN Spray A. Computed results are shown for a WSR model and a PDF method using the Euclidean minimum spanning tree (EMST) mixing model, for three different values of the mixing model coefficient (1.5, 2.5 and 10.0). Figure courtesy of S. Ferreyro-Fernandez, Penn State.

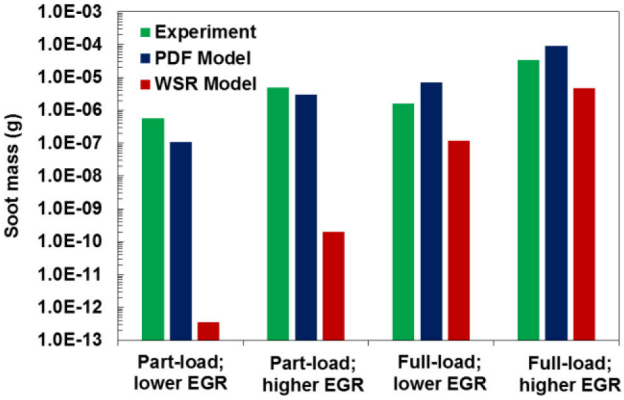

Figure 13. Computed engine-out soot mass and measured particulate mass for a heavy-duty diesel engine at four different operating conditions. Computed results are shown for a WSR model and a PDF model. The figure is based on data published in [7].

Fuel Mechanisms and the Improvement in Computational Speed

A second and important result of the modeling effort identified that increasingly large chemical mechanisms are needed to capture fuel effects on autoignition, especially when soot formation is also considered. In this project, significant progress has been made in improved stiff ODE solvers for combustion CFD [9]. The progress resulted from the recognition of two key issues that had received little attention earlier: the solver reinitialization problem that is inherent in combustion CFD (the need to stop/restart the solver on every CFD time step for every computational element), and the fact that the actual solution accuracy varies widely from one solver to another for the same values of the user-specified internal solver error tolerances. These observations led us to consider of a class of stiff ODE solvers based on extrapolation methods. Across a wide range of engine-relevant conditions, and for chemical mechanisms ranging in size from fewer than 50 to more than 5000 species, an extraploation solver provides significantly more accurate solutions at lower computational cost compared to the best available methods to date (Figure 14). High solution accuracy is essential to extract reliable conclusions regarding complex, and sometime subtle, fuel effects in engines.

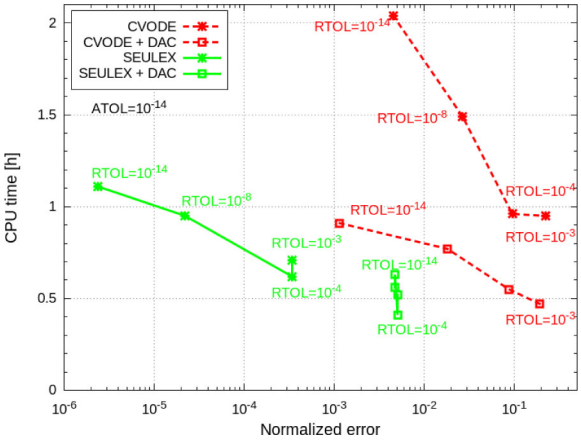

Figure 14. CPU time versus normalized error in computed OH volume fraction at the instant of peak heat release for a HCCI engine [9]. In all cases, the absolute error tolerance is ATOL = 10^{-14} and the relative error tolerance RTOL ranges from 10^{-14} to 10^{-3}. Results for a BDF solver (CVODE) and an extrapolation solver (SEULEX) are shown. Results with dynamic adaptive chemistry (DAC) also are shown.

Understanding Engine Processes through Scaled Experiments

The parameter space was also explored using laboratory scaled experiments that captured key fluid mechanic phenomena and allowed for high-speed visualization of fluid interaction with engine surfaces. These experiments were conducted using a gas jet experiment at the Pennsylvania State University, which has been scaled from engine-relevant conditions using methodologies described in Ref. [10]. In this study, gas jets are used to mimic diesel injection and make more detailed measurements of jet behavior in non-reacting environments. These jets have been studied in both high-pressure [11, 12] and low-pressure [13, 14] facilities, and with the proper scaling, both types of experiments can provide information about diesel injection processes. This scaling comes from momentum and mass conservation considerations, and authors including Naber and Siebers [15] and Pickett *et al.* [16] have described these scaling processes in detail. One significant benefit of using gas jets, particularly in low-pressure ambient environments, is that detailed measurement of jet processes is easier and the turn-over time between experiments is negligible compared to high-pressure, liquid-fueled systems. The fast data collection rate available in gas jet experiments is important for both fundamental studies of jet mixing behavior and applied studies, such as this one, where initial screening of injection schedules and geometries can be completed quickly.

The experimental setup for the gas jet experiments follows that of Abani and Ghandhi [13, 17]. The gas from the supply canisters is fed into a single injector through two fast-acting two-way solenoid valves. The valves are normally closed, and open when voltage is supplied by LabView and a National Instruments 9482 4-channel electromechanical relay module. The flow factor of the valve (Cv) is 0.76 and the response time is 5-10 ms. The valve pipe size is 1/8".

The gas jet is produced from an orifice in the center of the nozzle plate on the injector into quiescent air at ambient temperature and pressure. In all of the studies for the SuperTruck program, the orifice diameter is 1 mm.

Two diagnostics are used to determine the jet penetration and spreading. First, a z-type schlieren configuration [18] is used to visualize the flow. The jet-tip penetration and dispersion angle are determined from the schlieren images. Light is provided by a continuous LED. 6" parabolic mirrors are used on either side of the setup. High-speed images are captured with a Photron SA1.1 Fastcam. The camera has a viewing region that is 384 by 864 pixels for the multiple-injection studies and a viewing region that is 576 by 504 pixels for the bowl-wall impingement studies. The maximum height and width of the images from the multiple injection studies are 12.5 cm and 5.8 cm, respectively, providing a resolution of 65.5 pixels/cm. The resolution of the images in the bowl-wall impingement studies is approximately 47.5 pixels/cm. The images are recorded at 15 kHz.

Second, acetone planar laser-induced fluorescence (PLIF) is used to visualize jet penetration and spreading, and provide information about fuel concentration distributions. Acetone is seeded into the air using two acetone bubblers located between the regulators of the gas tanks and the valves of the injector body. An Edgewave pump laser at 532 nm and Sirah dye laser with Rhodamine 6G dye are used for acetone PLIF measurements. The pulse duration is 10 ns and the repetition rate for all PLIF tests in this study is 10 kHz. The power output of the UV laser beam typically ranges from 1 – 2.6 W and is tested daily using a Gentec UP25-H power meter. Images were acquired at 10 kHz using a Photron SA5 camera with a LaVision IRO intensifier. Details of the image processing for both techniques can be found in Refs. [10] and [19].

A series of schlieren and acetone tracer-PLIF experiments was conducted to determine the optimal bowl geometry and nozzle configuration for effective in-cylinder mixing. Optimal mixing was determined using a metric of "air utilization," or how well the jet fluid mixes with the ambient fluid. The mixing is determined both by concentrations from the PLIF measurements as well as quantification of the spatial extent of the jet fluid; for a given injection schedule, a larger spatial extent of the jet fluid indicates better fluid mixing and air utilization. The test matrix is shown in Table 1, which contains scaled values from the engine simulations discussed in the previous section; scaling used methodologies described in Ref. [10].

Table 1. Operating conditions for gas jet studies of two injector configurations, 51° (7-hole injector) and 45° (8-hole injector), with injection pressures and durations.

Angle between orifices (degrees)	Injection Pressure (kPa)	Experiment Injection Duration (ms)
51°	120	18
51°	130	16
51°	140	14
45°	120	18
45°	130	16
45°	140	14

The test matrix in Table 1 was repeated for two bowl designs, denoted Bowl 1 and Bowl 3, which were selected through the simulation optimization process discussed in the section above.

These two bowl shapes were tested in two different configurations, allowing for measurement of different flow processes. First, the bowl shape was extruded into a two-dimensional block, shown in Figure 15, which allowed for schlieren imaging of the jet flow along the contour of the bowl wall.

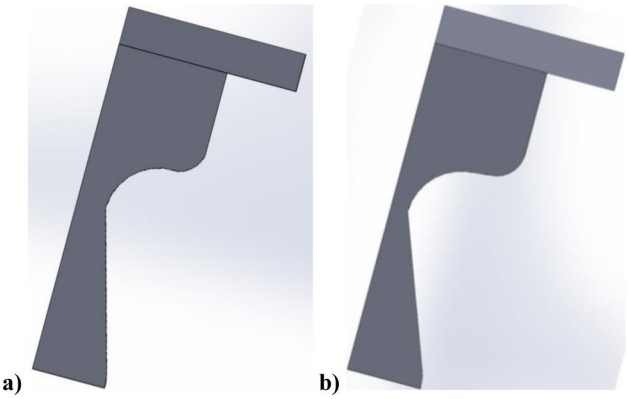

Figure 15. Two-dimensional extrusions of a) Bowl 1 and b) Bowl 3 used for schlieren imaging of jet interaction with bowl shape.

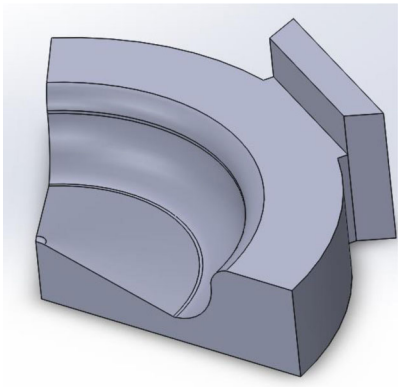

Figure 16. Three-dimensional rotation of Bowl 1 used for acetone-PLIF imaging of jet interaction with bowl surfaces.

Second, the bowl shape was rotated to make a sector of the bowl and the flow along the bowl was imaged from two angles using acetone-PLIF. This configuration is shown in Figure 16, where the bowl sector has a mounting plate attached to it on the top-right of the figure. Both the bowl shapes in Figure 15 and Figure 16 were fabricated using a 3D printer and are made from dark-colored plastic to reduce laser reflections.

The ensemble-averaged pressure curves for schlieren experiments are shown in Figure 17 for the test cases with two different nozzle configurations. The actual injection times for the experiments were longer than the calculated scaled injection times due to software and experimental response time limitations, so the calculated end of injection (EOI) times (14, 16, and 18 ms) are given by vertical dashed lines. The penetration and spreading angle after the scaled EOI time would be irrelevant, however, as in all cases the jets hit the bowl wall well before EOI. It is still necessary to only consider the motion of

fluid moving back until the scaled EOI and not after EOI. These results indicate that the injector pressure does not change significantly with the orifice hole angle, indicating that we can confidently compare the results from these two orifice configurations at all three pressures.

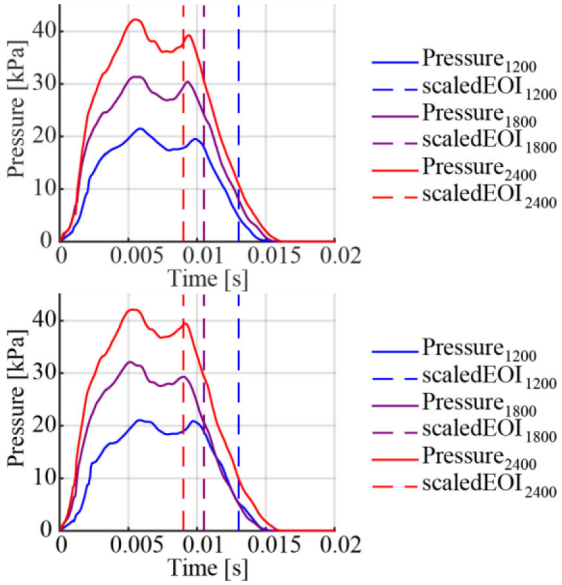

Figure 17. The ensemble-averaged pressure curves are shown for three gas jet schlieren experiments with a 51° nozzle spacing (top) and 45° nozzle spacing (bottom). The subscripts in the legend indicate the injector pressures in the engine (1200, 1800, and 2400 bar) which correspond to experimental injection pressures of 20, 30, and 40 kPa, respectively.

Results from both the extruded bowl as well as the rotated bowl experiments show that the penetration and spreading rates of the jets were similar for the two orifice angles, the two bowls, and the three pressures. The result is expected as the momentum of the jet coming from the orifice is large and the confinement from the bowl in the initial development of the jet is negligible. However, significant differences between bowl shapes and orifice angles are found in the measurements of jet interaction with the bowls.

Schlieren experiments of jet interaction with the extruded bowls show that Bowl 3 has better air utilization in the contour plane of the bowl. From qualitative observations of the fluid motion near the bowl wall, the deeper bowl in Bowl 3 appears to allow the fuel to spread more, resulting in better air utilization. In particular, fluid from the jet is recirculated in the bottom of the bowl and flows back towards the injector, along the bottom of the bowl. The fluid that interacts with the wall of Bowl 1 is likely diverted towards the squish region rather than back towards the nozzle. As the squish region of the engine has limited air for combustion and significant surface area for heat loss, it is more efficient from both a combustion and thermal perspective to encourage air recirculation towards the center of the combustion chamber rather than towards the edges.

The improvement in air utilization using Bowl 3 is also observed in the LIF results, as shown in Figure 19. The LIF images were recorded for a single plane through the centerline of the jets, where the camera is angled so that it can capture the motion of the jets inside the bowl. After the jets impinge on the bowl wall (at about 4 ms aSOI), it appears as though the jets are spreading wider, but this is likely due to fluid coming back from the bowl wall into the centerline plane of the jet as the two regions are somewhat disconnected. The increased quantity of acetone-seeded fluid around the edges of the jets appears to be more prevalent with the Bowl 1 geometry. It is possible that this occurs because after the jets interacts with the wall of Bowl 1, they move back towards the jet in this plane. However, after the jets interact with the wall of Bowl 3, they move back towards the nozzle along the bowl wall and the fluid is not pushed towards the jet as much, and it would not appear in the images taken in the plane along the centerline of the jets.

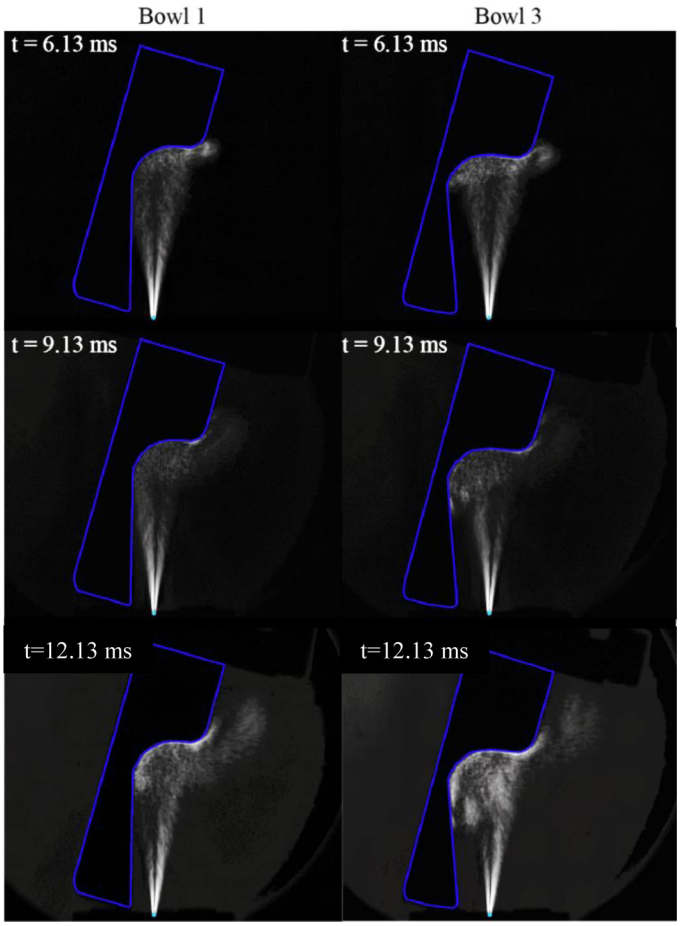

Figure 18. The schlieren images for gas jet tests with extruded Bowl 1 (left) and Bowl 3 (right) are shown for increasing time after SOI. The blue dot indicates the location of the injector orifice.

One metric that is used to understand the effects of jet angle (number of orifices), which is driven by jet-jet interaction, on mixing is the rate at which the acetone-seeded air moves back towards the nozzle after interacting with a wall. In the near nozzle region there were no obvious differences in the PLIF images when comparing images from tests with the same bowl shape and different injector orifice angles other than the spacing between the jets. However, in the region near the bowl wall there appeared to be more acetone-seeded fluid moving back towards the nozzle in the space between the jets in the configuration with a 51° angle between injector orifices (7-hole injector design) compared to a 45° angle between injector orifices (8-hole injector design), which is pointed out using a blue arrow in

Figure 19. An analysis of this penetration rate and other quantitative metrics is described in detail in Ref. [19]. The results of this testing showed that the 7-hole injector design also allows for better mixing.

A number of key lessons have been learned from this gas jet data. First, we have shown that the gas jet experiment is capable of capturing important differences between jet and bowl configurations, and allows for an optically-accessible experimental configuration to screen engine designs for their influence on fluid-mechanic processes. For this particular engine configuration, we show that the 7-hole injector together with the Bowl 3 design allows for superior air utilization, which can increase combustion efficiency, reduce thermal losses, and improve emissions.

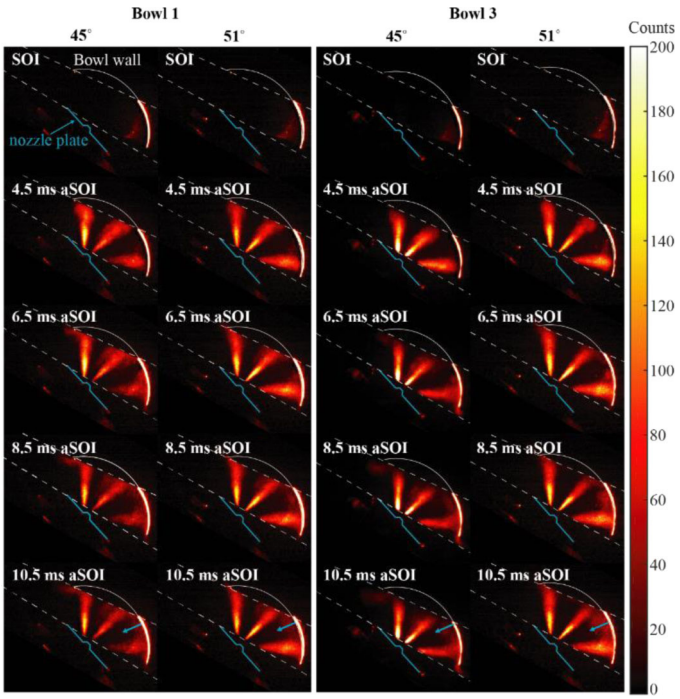

Figure 19. After the acetone-seeded jets of air interact with the bowl wall, more acetone-seeded fluid appears to move further back towards the nozzle in the images shown for the 51° spacing (7-hole injector configuration). The blue arrows show the direction the fluid is moving back (normal to the bowl surface). Dotted white lines indicate the location of the laser sheet.

OUTCOMES AND NEXT STEPS

The outcome of this work is an improved design strategy for exploring advanced combustion strategies that result in ultra-high efficiency and low emissions combustion. We have used a unique combination of 1-D and 3-D simulation, scaled experiments, and engine testing, to design and understand combustion processes in new engine geometries and at high-efficiency engine operating conditions. 1-D simulation, validated with 3-D simulation and engine testing, allowed for a DOE over a large parameter space, revealing combinations of operating conditions and engine geometries that achieve efficiency and emissions goals. High-fidelity 3-D simulation in conjunction with scaled fluid-mechanic experiments refined the piston-bowl design, and helped to identify combustion strategies that would reach the design goals. Engine data libraries throughout this process have helped to validate models and provide insight into the impact of design choices on engine performance. Finally, we plan to verify the outcome of the methods identified in this paper with research engine testing at the University of Michigan.

The design process has fulfilled the goal of the Department of Energy's SuperTruck program, where the path to 55% BTE was demonstrated through simulation and experiment. This exercise provides a foundation for work on the SuperTruck II program, where demonstration of a 55% BTE engine in dyno testing is required. The tools developed in this program, incorporated in the Volvo combustion CFD framework, and the lessons learned from this work will be invaluable to achieving goals in next-generation engine designs.

REFERENCES

1. U.S. Department of Energy, (2009) "Recovery act-systems level technology development, integration,and demonstration for efficient class 8 trucks (SuperTruck) and advanced technology powertrains for light-duty vehicles (ATP-LD)" DE-FOA-0000079
2. Kosters, A. and Karlsson A., (2016) "Validation of the VSB2 spray model against spray A and spray H" Atomization and Sprays, 26(8):775–798
3. Peters, N., (2000) *Turbulent combustion*, Cambridge university press,
4. "STAR-CD CFD," (http://mdx.plm.automation.siemens.com/star-cd)
5. "OpenFOAM," (http://openfoam.org/)
6. Haworth, D.C., (2010) "Progress in probability density function methods for turbulent reacting flows" Progress in Energy and Combustion Science, 36(2):168–259
7. Raj Mohan, V. and Haworth D.C., (2015) "Turbulence-chemistry interactions in a heavy-duty compression-ignition engine" Proceedings of the Combustion Institute, 35(5):3053–3060
8. *Engine Combustion Network (ECN)*. Available from: https://ecn.sandia.gov/ (2016)
9. Imren, A. and Haworth D.C., (2016) "On the merits of extrapolation-based stiff ODE solvers for combustion CFD" Combustion and Flame, in press
10. Borz, M., Kim, Y., and O'Connor, J., "The Effects of Injection Timing and Duration on Jet Penetration and Mixing in Multiple-Injection Schedules," SAE Technical Paper 2016-01-0856, 2016, doi:10.4271/2016-01-0856.
11. Bruneaux, G., Causse, M., and Omrane, A., "Air Entrainment in Diesel-Like Gas Jet by Simultaneous Flow Velocity and Fuel Concentration Measurements, Comparison of Free and Wall Impinging Jet Configurations," *SAE Int. J. Engines* 5(2):76–93, 2012, doi:10.4271/2011-01-1828.
12. Eismark, J., Hammas, M.vKarlsson A., Denbratt I., Davidson L., (2012) "Role of turbulence for mixing and soot oxidation for an equivalent diesel gas jet during wall interaction studied with LES", THEISEL, Valencia, Spain
13. Abani, N. and Ghandhi J.B., , (2012) "Behavior of unsteady turbulent starting round jets" Journal of Fluids Engineering, 134(6):061202
14. Atassi, N., Boree J., Charnay G., (1993) "Transient behavior of an axisymmetric turbulent jet" Applied Scientific Research, 51(1–2):137–142
15. Naber, J. and Siebers, D., "Effects of Gas Density and Vaporization on Penetration and Dispersion of Diesel Sprays," SAE Technical Paper 960034, 1996, doi:10.4271/960034.
16. Pickett, L., Caton J., Musculus M., Lutz A., (2006) "Evaluation of the equivalence ratio-temperature region of diesel soot precursor formation using a two-stage Lagrangian model" International Journal of Engine
17. Research, 7(5):349–370 Ghandhi, J.B., (2013) *Personal communication*,
18. Settles, G.S., (2012) *Schlieren and shadowgraph techniques: visualizing phenomena in transparent media*, Springer Science & Business Media,
19. Borz, M.J., *Gas jet studies for the characterization of advanced injection schedules and bowl designs in diesel engines*, Mechanical Engineering, Pennsylvania State University (2016)

CONTACT INFORMATION

Samuel McLaughlin
samuel.mclaughlin@volvo.com

ACKNOWLEDGMENTS

This work was sponsored by Volvo Technology of America and the U.S. Department of Energy under DOE award number DEEE0004232.

DEFINITIONS/ABBREVIATIONS

BSNOx - Brake specific NOx

BTE - Brake thermal efficiency

CCR - Critical compression ratio

CFD - Computational fluid dynamics

CFR - Cooperative Fuel Research

DAC - Dynamic adaptive chemistry

DOE - Design of experiments

ECN - Engine combustion network

EGR - Exhaust gas recirculation

EOI - End of injection

HCCI - Homogeneous charge compression ignition

ICE - Internal combustion engine

IMEP - Indicated mean effective pressure

LED - Light emitting diode

PDF - Probability density function

PLIF - Planar laser-induced fluorescence

PRF - Primary reference fuel

WSR - Well-stirred reactor

aSOI - After start of injection

mRIF - Multiple representative interactive flamelet